

Article

Reliability Analysis of RC Slab-Column Joints under Punching Shear Load Using a Machine Learning-Based Surrogate Model

Lulu Shen, Yuanxie Shen  and Shixue Liang * 

School of Civil Engineering and Architecture, Zhejiang Sci-Tech University, Hangzhou 310018, China

* Correspondence: liangsx@zstu.edu.cn

Abstract: Reinforced concrete slab-column structures, despite their advantages such as architectural flexibility and easy construction, are susceptible to punching shear failure. In addition, punching shear failure is a typical brittle failure, which introduces difficulties in assessing the functionality and failure probability of slab-column structures. Therefore, the prediction of punching shear resistance and corresponding reliability analysis are critical issues in the design of reinforced RC slab-column structures. In order to enhance the computational efficiency of the reliability analysis of reinforced concrete (RC) slab-column joints, a database containing 610 experimental data is used for machine learning (ML) modelling. According to the nonlinear mapping between the selected seven input variables and the punching shear resistance of slab-column joints, four ML models, such as artificial neural network (ANN), decision tree (DT), random forest (RF), and extreme gradient boosting (XGBoost) are established. With the assistance of three performance measures, such as root mean squared error (RMSE), mean absolute error (MAE), and coefficient of determination (R^2), XGBoost is selected as the best prediction model; its RMSE, MAE, and R^2 are 32.43, 19.51, and 0.99, respectively. Such advantages are also reflected in the comparison with the five empirical models introduced in this paper. The prediction process of XGBoost is visualized by SHapley Additive exPlanation (SHAP); the importance sorting and feature dependency plots of the input variables explain the prediction process globally. Furthermore, this paper adopts Monte Carlo simulation with a machine learning-based surrogate model (ML-MCS) to calibrate the reliability of slab-column joints in a real engineering example. A total of 1,000,000 samples were obtained through random sampling, and the reliability index β of this practical building was calculated by Monte Carlo simulation. Results demonstrate that the target reliability index requirements under design provisions can be achieved. The sensitivity analysis of stochastic variables was then conducted, and the impact of that analysis on structural reliability was deeply examined.

Keywords: reliability analysis; RC slab-column structure; machine learning; Monte Carlo simulation; shapley additive explanation



Citation: Shen, L.; Shen, Y.; Liang, S. Reliability Analysis of RC Slab-Column Joints under Punching Shear Load Using a Machine Learning-Based Surrogate Model. *Buildings* **2022**, *12*, 1750. <https://doi.org/10.3390/buildings12101750>

Academic Editors: Ming-Hung Hsu, Zheng-Yun Zhuang and Ying-Wu Yang

Received: 12 September 2022

Accepted: 18 October 2022

Published: 20 October 2022

Publisher's Note: MDPI stays neutral with regard to jurisdictional claims in published maps and institutional affiliations.



Copyright: © 2022 by the authors. Licensee MDPI, Basel, Switzerland. This article is an open access article distributed under the terms and conditions of the Creative Commons Attribution (CC BY) license (<https://creativecommons.org/licenses/by/4.0/>).

1. Introduction

Reinforced concrete (RC) slab-column structures comprised of slabs and columns are susceptible to punching shear, because the beams are not arranged for the considerations of structural layout under slabs [1]. Under excessive punching shear loads, the interior slab-column joint is usually destroyed first, the rest of the joints are destroyed in succession, and the progressive collapse of overall structure takes place [2]. Accidents (Figure 1), such as the collapse of a 16-storey apartment building [3] in Boston, US and Skyline Plaza [4] in Virginia, US, have caused severe damage, which arouse the researchers' attention regarding the reliability analysis of RC slab-column joints.

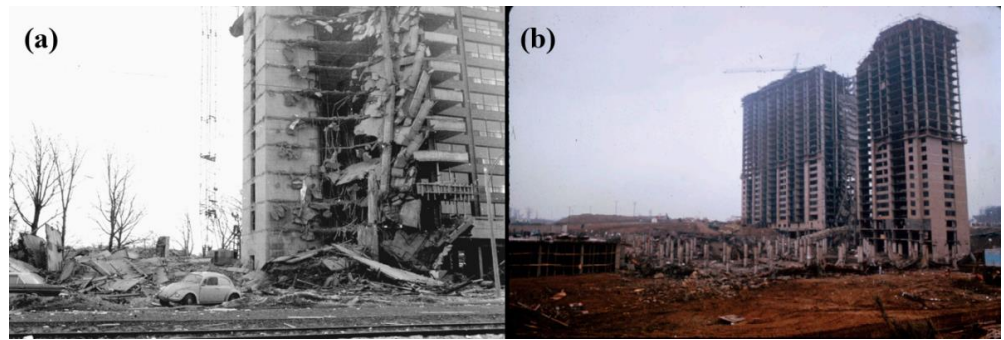


Figure 1. Collapse of slab-column structures: (a) a 16-storey apartment building, Boston [3]; (b) Skyline Plaza, Virginia [4].

To assess the performance of slab-column structures, especially the slab-column joints, a number of experimental studies have been conducted on the punching shear resistance. With the experimental results, some empirical models [5–15] have been proposed based on a variety of mechanical theories. Kinnunen and Nylander [5] analyzed the experimental data of circle slab-circle columns, and created the sector model. Based on this, Broms [6,7] proposed a modified model considering the impact of size effect, which obtained the solution of the ultimate angle of the slabs. Tian et al. [8] proposed a prediction model considering the impact of reinforcement strength (ρf_y). According to the eccentric shear stress model proposed by Stasio et al. [9], an improved model with stronger applicability was proposed by Moe [10], which became the theory basis of both GB 50010-2010 [11] and ACI 318-19 [12]. After analyzing the critical cracks of slab-column joints and considering the impact of aggregate size, the critical shear crack theory (CSCT) was proposed by Muttoni [13]. Based on the modified compression field theory (MCFT), Wu et al. [14] developed a prediction model; its prediction performance was validated by many experimental data. According to the regression analysis of the experimental data, a prediction model was proposed by Chetchotisak et al. [15].

However, the aforementioned mechanical or empirical models possess the problem of prediction precision [16,17]. As a typical data-driven model with advantages such as superior prediction performance and high computational efficiency, machine learning (ML) is applied to many engineering fields successfully [18–25]. In the resistance prediction of slab-column joints, Nguyen et al. [16] established a prediction model using extreme gradient boosting (XGBoost), the performance of which was validated by empirical models and other two ML models. Mangalathu et al. [17] also constructed XGBoost models, and used SHapley Additive exPlanation (SHAP) to illustrate the prediction process of XGBoost. Shen et al. [23] established an ML model to predict the punching shear resistance of fiber-reinforced polymer (FRP)-reinforced concrete slabs, the performance of which was better than that of the compared empirical models. Truong et al. [24] studied the punching shear strength of FRP-RC slab column connections with the assistance of ML models.

The objective of reliability analysis is to evaluate the safety of structures by considering how their performances are affected by the uncertainties, which are introduced by random material properties or stochastic loads [26]. There are two types of methods for reliability analysis, namely the gradient-based method and the simulation-based method [27]. The first method contains the first-order reliability method (FORM), and the second-order reliability method (SORM) aims to find the most likely failure point through the limit state function estimation. Such a method has a high computational efficiency, but it introduces approximations that are sometimes unacceptable from a precision point of view [28]. As the main simulation-based method, the Monte Carlo sampling method is conventional, clear, and easy to use, but such a method requires numerous samples [29,30]. Nassim et al. [31] studied the reliability of two cases by using the response surface method (RSM) as well as Monte Carlo simulation (MCS). Olmati et al. [32] proposed a simplified analysis framework and used MCS to analyze the reliability of an office building. Chetchotisak et al. [15]

studied the structural reliability within two kinds of concrete (normal-strength concrete and high-strength concrete) by using MCS. Ricker et al. [33] utilized three reliability analysis techniques, such as the mean-value first-order second moment method (MVFOSM), the first-order second moment method (FOSM), and MCS, to assess the safety levels of the punching shear resistance of flat slabs without shear reinforcement. However, the relatively low prediction accuracy of the aforementioned mechanical or empirical models led to unsatisfying results of the reliability analysis. To obtain more accurate reliability analysis results, the finite element method (FEM) is popularly applied as the surrogate model of structural response under stochastic material properties or loading conditions [34]. The complexity and nonlinearity existing in structures, as well as the randomness produced by influential factors of a structure itself, prove that FEM becomes a fine choice. However, the mechanical property-based analysis restricts the computational efficiency of FEM, which is inapplicable to practical projects [35]. Furthermore, as the most commonly used parallel analysis method in a stochastic context, MCS has a problem of inadequate computational efficiency, because the number of samples needed for analysis is considerably large [36]. The ML model is a prospective solution for the contradiction between computational efficiency and accuracy, and has been applied in the reliability analyses of RC structures in the latest studies [37].

To the best knowledge of the authors, there is no available example combining reliability analysis of RC slab-column joints and ML; thus, this paper establishes an ML-MCS model for reliability analysis to meet the requirements of practical projects. The candidate ML models selected in this paper are artificial neural network (ANN), decision tree (DT), random forest (RF), and XGBoost. The final prediction model is screened from these four ML models, and the performance comparison between them is implemented through three performance measures: root mean squared error (RMSE), mean absolute error (MAE), and coefficient of determination (R^2). To display the advantages of the ML models, two design provisions (GB 50010-2010 [11] and ACI 318-19 [12]), as well as three prediction models proposed by Tian et al. [8], Wu et al. [14], and Chetchotisak et al. [15], are used for prediction performance comparison with ML models. Furthermore, SHAP is introduced for model explanation and analysis of influential factors; the prediction process can be visualized to facilitate the understanding [22]. Based on the established ML model, a slab-column structure in an actual engineering application is used for reliability analysis through MCS. Moreover, the safety assessment of the structure is discussed through sensitivity analysis.

2. Punching Shear Resistance Database of RC Slab-Column Joints

The high-fidelity data is the basis of the construction of ML models, so that the compilation of the experimental database is required. The punching shear resistance database containing 610 experimental data is shown in Appendix A, and the statistic information of input variables is listed in Table 1. Some relevant studies [8,14,38] report that there are seven main influential factors affecting slab-column joints: cross-section shape of column (s), cross-section area of column (A), slab's effective depth (d), compressive strength of concrete (f'_c), yield strength of reinforcement (f_y), reinforcement ratio (ρ), and span-depth ratio (λ). Their distributions are described in four measures: minimum, maximum, standard deviation, and average. The cross-section of each column has three shapes: square ($s = 1$), circle ($s = 2$), and rectangle ($s = 3$). The prediction target of the ML models is the punching shear resistance (V) of slab-column joints.

Table 1. Statistic information of input variables.

Parameter	Minimum	Maximum	Standard Deviation	Average	Type
s	1.00	3.00	0.58	1.40	Input
A (cm ²)	20.43	6375.87	596.68	489.31	Input
d (mm)	29.97	668.50	58.52	113.74	Input
f'_c (Mpa)	9.40	130.10	18.56	35.39	Input
f_y (Mpa)	234.70	749.00	115.83	456.60	Input
ρ (%)	0.25	7.31	0.70	1.26	Input
λ	0.61	32.51	4.83	6.59	Input
V (kN)	24.00	4915.00	406.56	403.25	Output

The histograms displayed in Figure 2 show the relative frequency distributions of the input variables and the output, and the red lines represent the cumulative distribution functions (CDF) of the parameters. To further understand the correlations between the input variables, they are quantified as a Pearson correlation coefficient matrix and shown in Figure 3, where coefficients represent the degree of linear correlation between input variables [39]. The coefficients close to -1 or 1 represent the obvious negative or positive linear correlation, and the degree of linear correlation between A and d is highest.

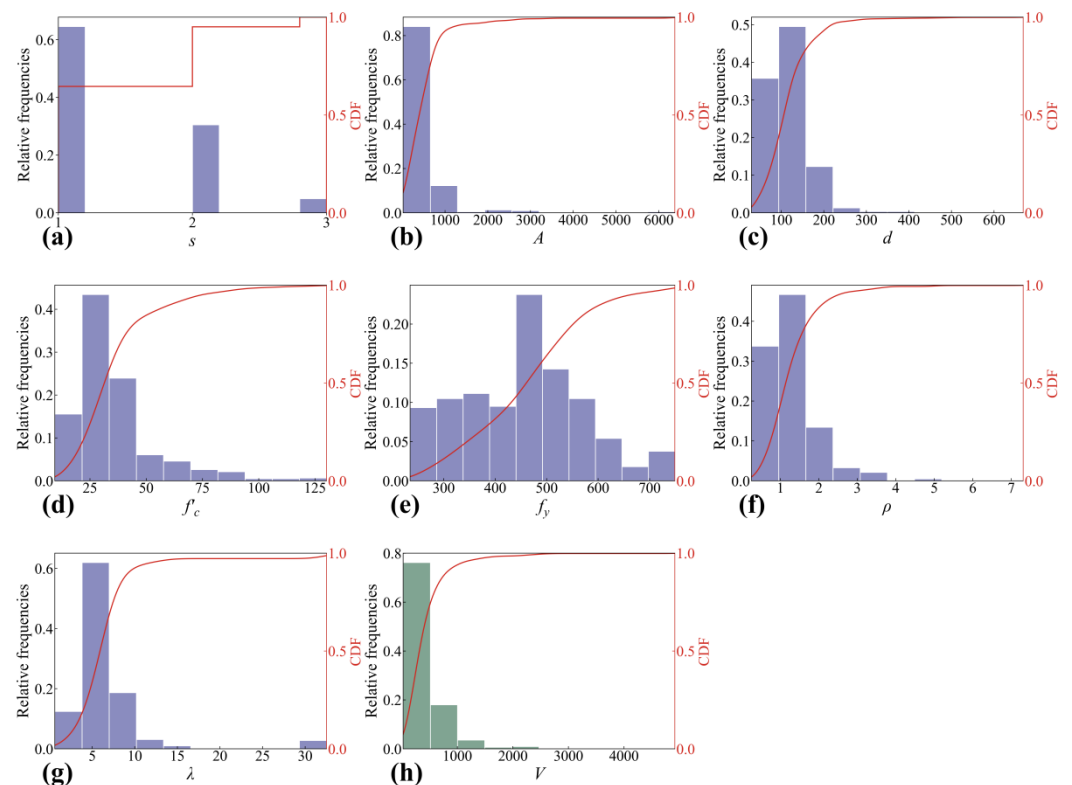


Figure 2. Distributions of the parameters in the database: (a) s ; (b) A ; (c) d ; (d) f'_c ; (e) f_y ; (f) ρ ; (g) λ ; (h) V .

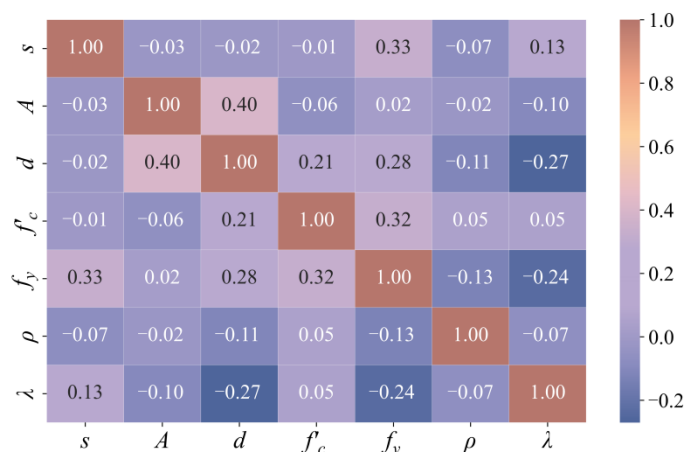


Figure 3. Correlation coefficient matrix of input variables.

3. Machine Learning Model for Punching Shear Resistance Prediction

The flow of establishment of an ML model is shown in Figure 4, which can be generalized as the following steps [40]: (1) Divide the compiled database as a training set (containing 500 data) and test set (containing 110 data) based on the ratio of 80% and 20%; (2) obtain the optimal hyperparameters by model training; (3) examine the generalization ability of the candidate model by the test set; (4) output the final prediction model. The four ML models selected in this paper are all established following this procedure, and the related introductions for models are displayed in Section 3.1.

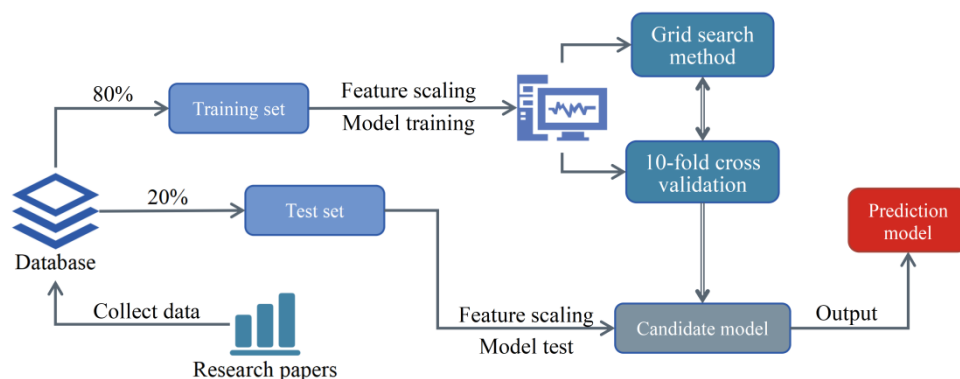


Figure 4. Flowchart of ML modelling.

3.1. Overview of Machine Learning Models

As the basic ML algorithms, ANN and DT have been widely studied and thus become the beginning of two types of artificial intelligence algorithms: deep learning and ensemble learning [41]. Among ensemble learning algorithms, RF and XGBoost are two representative algorithms constructed by different ensemble tactics such as bagging and boosting [40]. Due to the four typical ML models possessing different fitting techniques, the comparison of them enhances the credibility of the final prediction model.

Extreme Gradient Boosting

Extreme gradient boosting (XGBoost) inherits the combination strategy of gradient boosting decision tree (GBDT) and becomes the advanced implementation of the latter [42]. The employ of two regularization coefficients and the optimization of the second-order Taylor approximation guarantees not only the generalization ability, but also the prediction accuracy. The complexity of each base learner can be defined as:

$$\Omega(f_t) = \gamma T + \frac{1}{2} \lambda' \|w'\|^2 \tag{1}$$

where γ and λ' are the L1 and L2 regularization coefficients; T is the number of base learners; w' is the score of the node. Based on the fitting of the residuum of the prediction result, the prediction error of XGBoost can be further decreased. The fitting objective of each base learner can be formulated as:

$$\mathcal{L}(\varphi) = \sum_i l(y_{\text{pred}}^{(i)}, y^{(i)}) + \sum_k \Omega(f_k) \quad (2)$$

where l is the loss function; y_{pred} is the prediction value of the sample; y is the true value of the sample. Based on these, a prediction value generated by XGBoost can be expressed as the linear addition of the prediction values of all the base learners:

$$y_{\text{pred}} = \sum_{k=1}^K f_k \quad (3)$$

where K is the number of base learners.

3.2. Prediction Results of Machine Learning Models

The optimal hyperparameters of each ML model are obtained through the grid search method and through 10-fold cross-validation [43], which are listed in Table 2. To compare the prediction performances of different ML models, three performance measures, root mean squared error (RMSE), mean absolute error (MAE), and coefficient of determination (R^2), are adopted and expressed as:

$$\text{RMSE} = \sqrt{\frac{1}{m} \sum_{i=1}^m (y_{\text{pred}}^{(i)} - y^{(i)})^2} \quad (4)$$

$$\text{MAE} = \frac{1}{m} \sum_{i=1}^m |y_{\text{pred}}^{(i)} - y^{(i)}| \quad (5)$$

$$R^2 = 1 - \frac{\sum_{i=1}^m (y_{\text{pred}}^{(i)} - y^{(i)})^2}{\sum_{i=1}^m \left(y^{(i)} - \frac{1}{m} \sum_{i=1}^m y^{(i)} \right)^2} \quad (6)$$

where m is the number of samples.

Table 2. Optimal hyperparameters of ML models.

ML Model	Optimal Hyper-Parameter
ANN	Learning rate = 0.1, neurons number of hidden layer = 17, maximum iteration = 2000
DT	Maximum depth = 8
RF	Number of weak learner = 100, maximum depth = 14
XGBoost	Number of weak learners = 100, learning rate = 0.5, maximum depth = 3, $\gamma = 0.9$, $\lambda' = 1.4$

After the determination of the optimal hyper-parameters, four ML models are all established. To examine the prediction performance of ML models, five empirical models containing two design provisions [11,12], two mechanical models [8,14], and a regression analysis-based model [15] are introduced and listed in Table 3. Their prediction results are shown in Figure 5, where gray-green and blue-pink represent the prediction results of empirical models and ML models in the training set and the test set, respectively. XGBoost has the highest prediction accuracy, which indicates that XGBoost has been well-trained and possesses the best generalization ability. Such a conclusion is also in line with that of some studies [17,44]. RF and DT also have good prediction performance; their prediction tactics are suitable for the regression analysis of the punching shear resistance of RC slab-column joints [45]. However, the prediction performance of ANN must be improved; its

characteristic of a nonconvex function suggests that the obtained optimal solution is often local rather than global [18]. Utilizing the good fitting ability of the regression analysis method, the prediction model proposed by Chetchotisak et al. [15] has the best prediction result, but its credibility is low due to its lack of theoretical derivation. The prediction values of mechanical models proposed by Tian et al. [8] and Wu et al. [14] have a large deviation with true punching shear resistance, where coefficients reflected the relationships between influential factors and where punching shear resistance must be further modified. Furthermore, the prediction results of design provisions such as GB 50010-2010 [11] and ACI 318-19 [12] skew conservative; the prediction accuracy must be improved.

Table 3. Empirical models used for prediction performance comparison.

Empirical Model	Punching Shear Resistance Calculation Equation
GB 50010-2010 [11]	$V_1 = 0.7\beta_h f_t \eta b_{0,0.5d} d; \eta = \min \begin{cases} \eta_1 = 0.4 + \frac{1.2}{\beta_s} \\ \eta_2 = 0.5 + \frac{\alpha_s d}{4b_{0,0.5d}} \end{cases}$
ACI 318-19 [12]	$V_2 = \min \left[\frac{1}{3}, \frac{1}{6} \left(1 + \frac{2}{\beta_s} \right), \frac{1}{12} \left(2 + \frac{\alpha_s d}{b_{0,0.5d}} \right) \right] \lambda_s \sqrt{f'_c} b_{0,0.5d} d; \lambda_s = \sqrt{\frac{2}{1+0.004d}} \leq 1$
Tian et al. [8]	$V_3 = 0.65\zeta A_c (\rho f_y \sqrt{f'_c})^{\frac{1}{2}}; \zeta = \sqrt{\frac{d}{c}}; A_c = 4(c+d)d$
Wu et al. [14]	$V_4 = 0.00040(\rho)^{\frac{1}{5}} b_{0,2d} d L \sqrt{f'_c} / \left(0.31 + \frac{24\omega}{a_d + 16} \right); \omega = 0.0005 \frac{0.9d}{\sin\theta}; a_d = 20; \theta = 45^\circ$
Chetchotisak et al. [15]	$V_5 = 92.43(f'_c)^{1.21} \left(\frac{1}{100\rho} \right)^{1.47} (b_{0,0.5d})^{0.42} d^{1.35} k^{4.66}; k = \sqrt{(np)^2 + 2(np)} - (np);$ $n = E_s / E_c = 2 \times 10^5 / 4700 \sqrt{f'_c}$

β_h is the sectional depth influence coefficient; f_t is the design value of the tensile strength of concrete; $b_{0,0.5d}$ is the critical section perimeter at a distance of $0.5d$ away from the column; β_s is the ratio of the long side to the short side of the column; α_s is the influential coefficient of the column type (40 for interior columns); c is the column size; $b_{0,2d}$ is the critical section perimeter at a distance of $2d$ away from the column; L is the perimeter of the column.

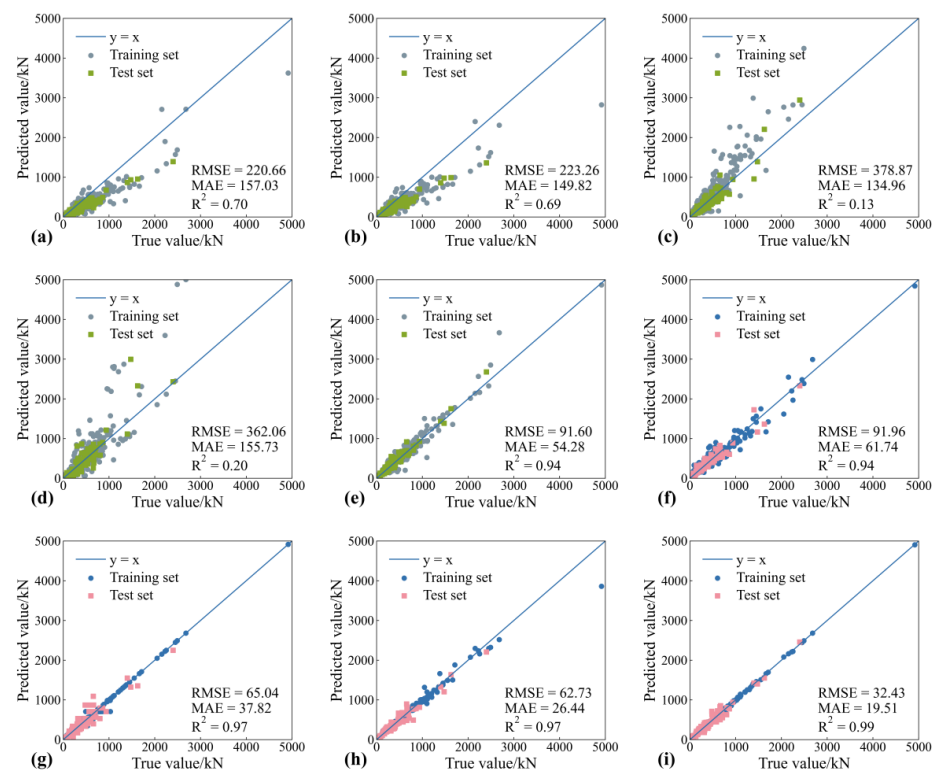


Figure 5. Scatter plots of the prediction results of the empirical models and the ML models: (a) GB 50010-2010; (b) ACI 318-19; (c) Tian et al.; (d) Wu et al.; (e) Chetchotisak et al.; (f) ANN; (g) DT; (h) RF; (i) XGBoost.

3.3. Interpretation of the ML Prediction Model

According to the performance comparison of the ML models in Section 3.2, XGBoost can be regarded as the final prediction model with the best prediction performance. The feature importance sorting produced by the built-in method of XGBoost [46], as shown in Figure 6, d has the greatest influence on punching shear resistance. However, this method can only provide the importance of influential factors; the effect tendency is unknown yet. Therefore, SHAP is introduced in this paper and utilized for model interpretation.

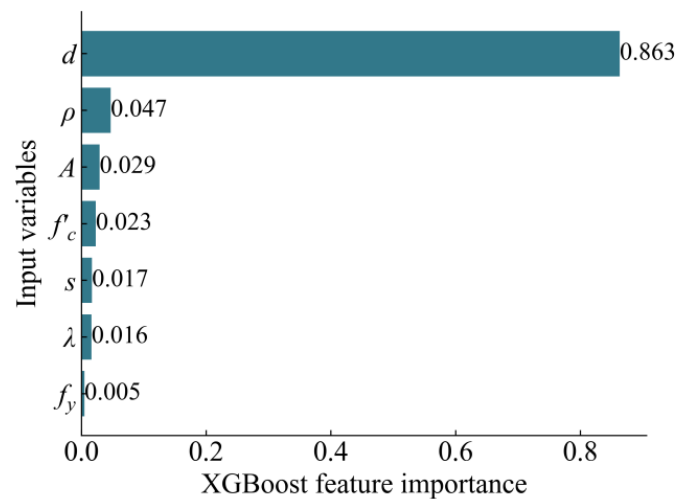


Figure 6. Importance sorting using XGBoost feature importance.

3.3.1. Overview of Shapley Additive Explanation

SHapley Additive exPlanation (SHAP) is useful for illustrating the prediction process of any ML model; it originates from the game theory and was proposed by Lundberg et al. [47,48]. For each prediction value, it can be formulated as the linear addition of the baseline value y_{base} and the SHAP value of each feature $f(x)$:

$$y_{\text{pred}}^{(i)} = y_{\text{base}} + \sum_{j=1}^n f(x_{ij}) \quad (7)$$

where n is the number of features. The quantified contribution of the feature is calculated through:

$$f(x_{ij}) = \sum_{S \subseteq N \setminus \{j\}} \frac{|S|!(M - |S| - 1)!}{M!} [f_x(S \cup \{j\}) - f_x(S)] \quad (8)$$

where N is the M -dimensional set containing all of the features; S is the $|S|$ -dimensional subset extracted from N ; $f_x(S \cup \{j\})$ is the prediction calculated through set S and feature j ; $f_x(S)$ is the prediction calculated through set S .

3.3.2. Model Interpretation Using Shapley Additive Explanation

The importance sorting provided by SHAP is shown in Figure 7, which is calculated by sum of the SHAP values of each sample. The feature importance sorting provided by SHAP is similar to that provided by XGBoost, but they conflict on the impact of s . Figure 7b shows the impact of each feature on punching shear resistance as positive or negative, and a feature can be regarded as the positive influential factor if the color of dot transforms from blue to red with the increase of the SHAP value. It can be seen that d , ρ , A , f_c , f_y , and s have positive impacts on resistance, and λ has a negative impact on resistance, which is consistent with some experimental studies [49–52]. Based on the importance sorting shown in Figure 7, the global impact of each influential factor is revealed, i.e., SHAP explains the global prediction process of XGBoost.

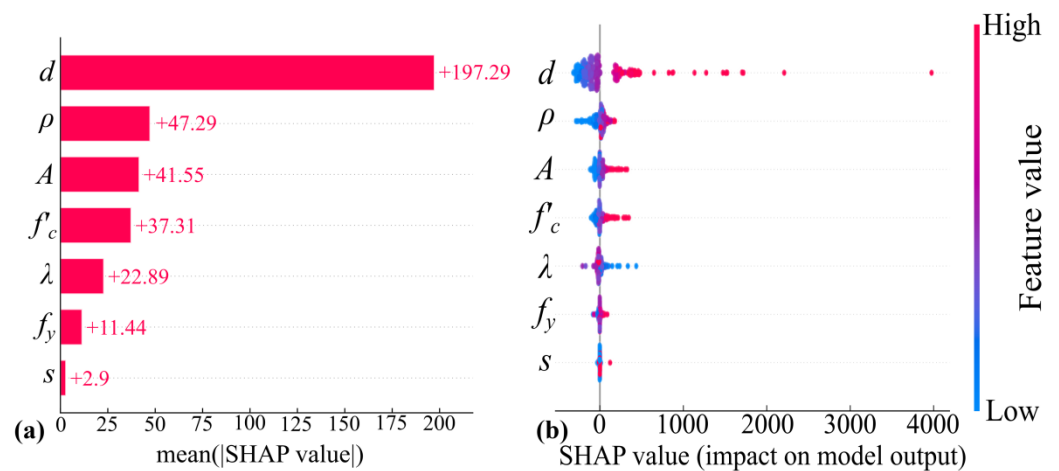


Figure 7. Global interpretation of punching shear resistance: (a) feature importance sorting; (b) SHAP value summary plot.

Figure 8 provides further insight for the impact of influential factors in the form of dependency plots, where the secondary axis represents the input variable interacting most frequently with the variable displayed in the x-axis. According to the variation range of the SHAP values, d and s have the greatest and least impacts, respectively, on punching shear resistance, which is consistent with the findings expressed by Figure 7a. Furthermore, the interaction between input variables is too complicated, such that the simple linear relationship cannot be used to represent it.

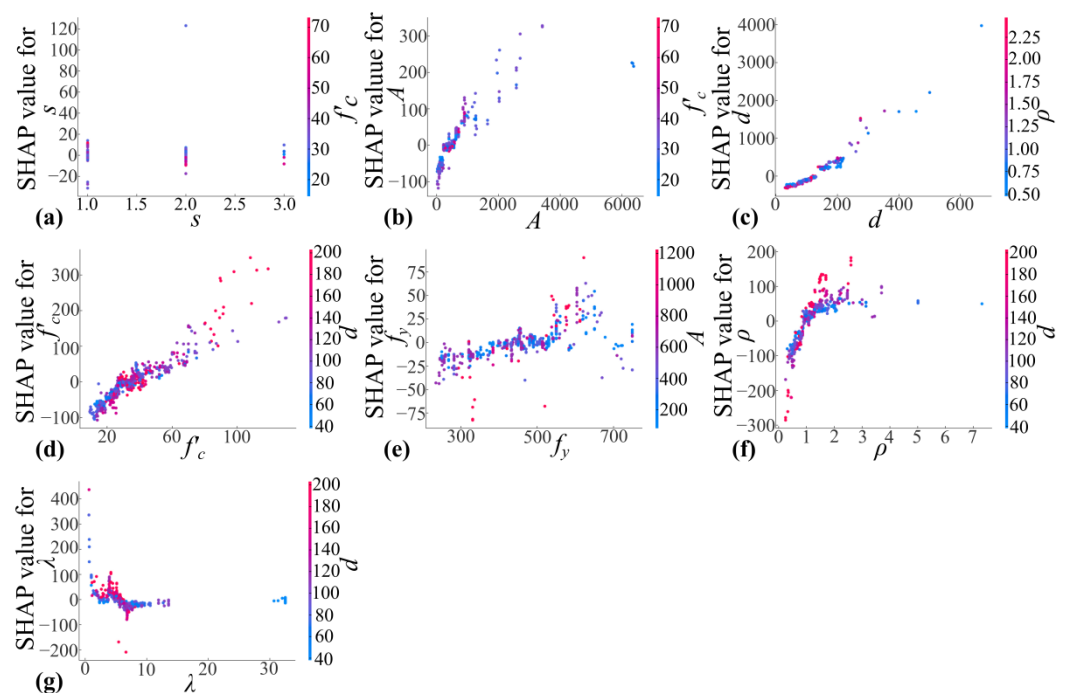


Figure 8. Feature dependencies of influential factors: (a) s ; (b) A ; (c) d ; (d) f_c ; (e) f_y ; (f) ρ ; (g) λ .

4. Reliability Analysis: RC Slab-Column Joint of an Office Building

The prototype building used for reliability analysis is a 7-story, 5-span RC slab-column shear wall office building [53], and it was designed using GB 50010-2010 [11] and GB 50011-2010 [54]. The building itself contains 3 m storey height and is supported by a 7.5 m \times 7.5 m column grid, and the interior joint shown in Figure 9 is selected as the study object. The selected joint consists of a slab with an effective depth of 209 mm and a square

column with side length of 530 mm, which is subjected to the specified dead load of 7.0 kN/m² and live load of 2.0 kN/m². According to the requirement of GB 50068-2018 [55], the dead load and live load used for limit state design must be adjusted by multiplying the partial safety factors for the load, such as 1.3 and 1.5. Therefore, the limit state function Z of structure can be defined as:

$$Z = R - 1.3S_G - 1.5S_Q \tag{9}$$

where R is the punching shear resistance; S_G is the dead load; S_Q is the live load. Furthermore, the measured compressive strength of C50 concrete in the slab is 39.31 Mpa, and the measured yield strength of HRB400 reinforcement is 421 Mpa. The reinforcement ratio of the joint is 0.81%, and the main influential factors are listed in Table 4.

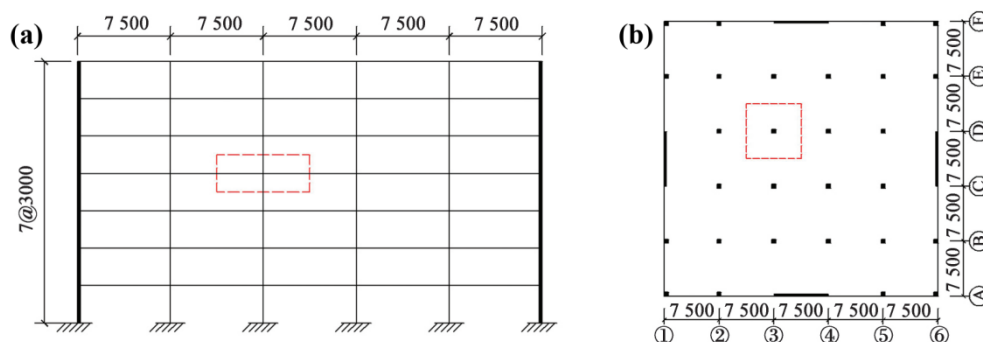


Figure 9. Prototype building [53]: (a) elevation; (b) plan.

Table 4. Main influential factors of the selected interior joint.

s	A/cm^2	d/mm	f'_c/Mpa	f_y/Mpa	$\rho/\%$	λ
1	2809	209	39.31	421	0.81	16.67

The statistic information and suitable probability density functions of the stochastic variables used for reliability analysis are listed in Table 5 [33,56], where COV is the coefficient of variance. According to the study conducted by Chojaczyk et al. [27], the COV of failure probability P_f calculated by MCS is accepted when its value is around 0.1; then the P_f around 10^{-4} (the normal failure probability of an existing structure) can be calculated through the simulation based on N samples [57]:

$$\text{COV}(P_f) = \frac{1}{P_f} \sqrt{\frac{(1 - P_f)P_f}{N}} \tag{10}$$

where N signifying 1,000,000 can be determined according to the aforementioned conditions. Another method used in the study conducted by Hadianfard et al. [58] stipulates that the number of samples needed for MCS can be determined through:

$$N > \frac{-\ln(1 - C)}{P_f} \tag{11}$$

where C is the confidence level, with values of 0.95 in this paper. Equation (11) suggests that the number of samples should not be less than 30,000, so that the value range calculated by Equations (10) and (11) is determined between 30,000 and 1,000,000. In this range, the variation of COV of failure probability P_f within 10 simulations is shown in Figure 10. The COV of failure probability decreases with the increase of the sample size from 30,000 to 1,000,000, which means that the result of the reliability analysis increasingly stabilizes.

Based on this knowledge, 1,000,000 samples are produced randomly and conducted for reliability analysis by XGBoost and MCS.

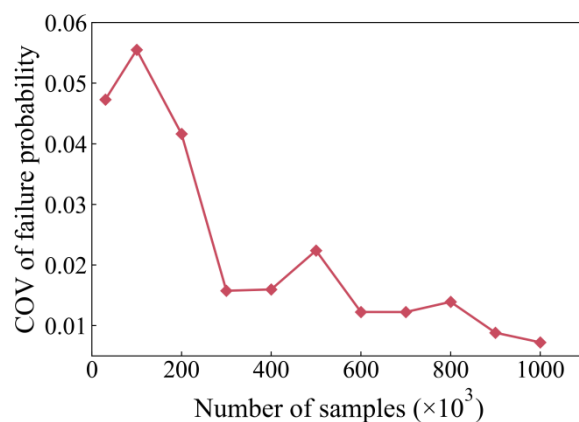


Figure 10. Effect of sample size on COV of failure probability.

Table 5. Stochastic variables used for Monte Carlo simulation.

Parameter	Average	Standard Deviation	COV	Distribution
d : slab's effective depth (mm)	209	6.27	0.03	Gaussian
f'_c : compressive strength of concrete (Mpa)	39.31	4.32	0.11	Gaussian
f_y : yield strength of reinforcement (Mpa)	421	33.68	0.08	Gaussian
S_G : dead load (kN)	393.75	27.56	0.07	Gaussian
S_Q : live load (kN)	112.5	32.4	0.288	Gumbel

4.1. Results of Structural Reliability Analysis

The efficient implementation of Monte Carlo simulation (MCS) is restricted by the sample size and the computational efficiency of the surrogate model [59], but this can be solved by XGBoost. The average computation time for 1,000,000 samples and the reliability analysis of the slab-column joint is 30 s. This is done by a laptop with four-core CPU and 8 GB memory, which demonstrates the efficiency of ML-MCS. Based on the regression prediction of punching shear resistance, the distribution and CDF of structural resistance are shown in Figure 11. The average and standard deviations of the distribution of structural resistance are 955.96 kN and 52.42 kN, respectively. MCS can estimate the failure probability of a structure effectively by calculating the probability of $Z < 0$ in Equation (9), and the related reliability analysis can also be realized. Table 6 displays the result of reliability analysis, where P_f is the failure probability of the structure; β is the reliability index; α_R and α_S are the sensitivity coefficients of resistance and load; r^* and s^* are the coordinates of the design point. The reliability index β indicates that the reliability and safety of the selected interior joint are good and meet the requirement of GB 50068-2018 [55].

Table 6. Results of reliability analysis.

P_f	β	α_R	α_S	r^*	s^*
0.00546	3.443	−0.655	0.755	837.625	837.625

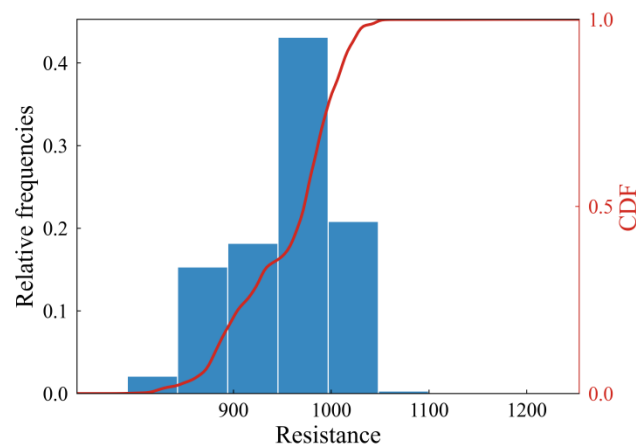


Figure 11. Distribution of structural resistance.

4.2. Sensitivity Analysis

The relationship between structural reliability and stochastic variables can be examined through sensitivity analysis [60]. The reliability index of the structure in the other two stochastic contexts (the stochastic structural resistance and stochastic loading condition) is shown in Figure 12. The reduction of the randomness of structural resistance or loading conditions can improve the reliability index, and the safety and stability of the structure also can be enhanced.

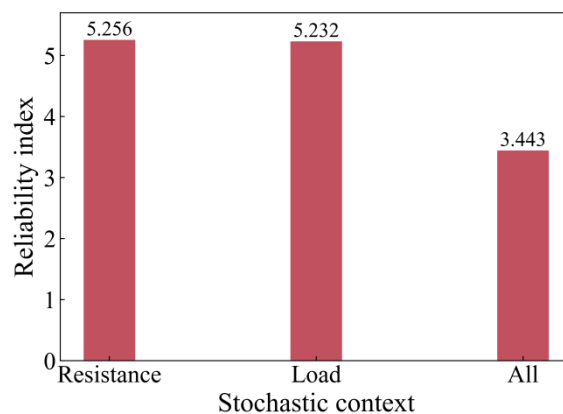


Figure 12. The reliability index in different stochastic contexts.

To study the impact of stochastic variables such as d , f'_c , f_y , and S_Q , their multiples are changed and their relationship with the reliability index is shown in Figure 13. The reliability index can be improved effectively with the increase of f'_c and f_y or the decrease of S_Q . However, there exists a complex relationship between slab depth d and reliability index; the reliability index is reduced when the multiple of d is between 1.15 and 1.35. The distribution of structural resistance with $1.3d$ is shown in Figure 14, which can be used to understand the reason for the reduction of the reliability index. The discontinuous distribution of structural resistance is existed, and the transition of failure modes from flexure to punching shear may exist, both through experimental and theoretical observations [22,61–63]. Therefore, the standard deviation of structural resistance is large, and the reliability index calculated by that is small.

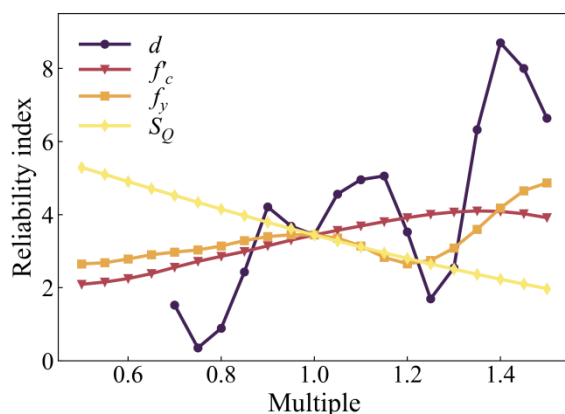


Figure 13. Impact of stochastic variables with different multiples on reliability index.

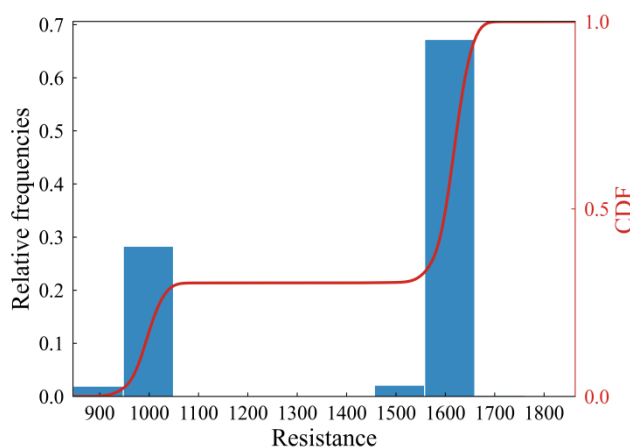


Figure 14. Distribution of structural resistance with 1.3d.

5. Conclusions

Structural reliability reflects the safety and stability of the entire practical structure subjected to permanent action and variable action [36], the calculation of which, through MCS, is restricted by the computational efficiency of the surrogate model. This work presents a framework for integrating the machine learning-based surrogate model into a Monte Carlo simulation to perform the reliability analysis with a satisfying accuracy and efficiency. An ML model is established and screened from four candidate ML models: as ANN, DT, RF, and XGBoost; the prediction performances of these are examined through three performance measures such as RMSE, MAE, and R^2 . Furthermore, the advantages of ML models are embodied by comparison with five empirical models. The final prediction model is used as the surrogate model of MCS, and an RC slab-column joint in an actual structure is introduced as the object of reliability analysis. The following conclusions can be drawn from this paper:

The punching shear resistance of RC slab-column joints is influenced mainly by seven influential factors: s , A , d , f'_c , f_y , ρ , and λ [38]. The capture of the mapping relationship between them can guarantee the construction of the ML model. With the help of the grid search method and 10-fold cross validation, four ML models with optimal hyperparameters are established. After comparison, XGBoost has the best prediction performance reflected in RMSE, MAE, and R^2 , and is selected as the final prediction model and used for reliability analysis.

To facilitate the understanding of the prediction process of ML, SHAP is utilized to quantify the contribution of input variables to punching shear resistance, and to visualize the prediction process. According to the importance sorting of input variables, d and s have the greatest and least impacts, respectively, on punching shear resistance. Furthermore,

feature dependency plots display the specific impact of each input variable by marginalizing the impacts of other variables. The analysis of the influential factors provides not only the understanding of prediction process, but also the suitable optimization sorting in structural design.

The actual structure adopted for the case study is an RC slab-column shear wall office building. The punching shear resistance of 1,000,000 samples produced by random sampling is calculated through XGBoost. The reliability analysis of the interior joint selected from the prototype building is conducted through MCS, and the final reliability index β meets the requirement of the design provisions of GB 50068-2018 [55]. Moreover, the sensitivity analysis reveals the impact of the stochastic context and the values of stochastic variables on structural reliability. Based on these, the computational efficiency of the reliability analysis of the slab-column joints can be enhanced on the premise of high computational accuracy. In future reliability analysis, some advanced sampling methods, such as Latin hypercube sampling and importance sampling, can be used to reduce the number of simulations appropriately. Furthermore, a program with some input windows of influential factors can be designed as a practical tool for reliability analysis.

Author Contributions: Conceptualization, L.S. and S.L.; software, L.S. and Y.S.; validation, L.S., Y.S. and S.L.; formal analysis, L.S.; writing—original draft preparation, Y.S.; writing—review and editing, S.L.; visualization, Y.S.; supervision, L.S. and S.L.; project administration, S.L. All authors have read and agreed to the published version of the manuscript.

Funding: This research was funded by Science Foundation of Zhejiang Province of China, grant number LY22E080016; National Science Foundation of China, grant number 51808499; Science Foundation of Zhejiang Sci-Tech University (ZSTU), grant number 19052460-Y; and the Education of Zhejiang Province, grant number 20050061-F.

Institutional Review Board Statement: Not applicable.

Informed Consent Statement: Not applicable.

Data Availability Statement: Not applicable.

Acknowledgments: This study is supported by the Engineering Research Centre of Precast Concrete of Zhejiang Province. The help of all members of the Engineering Research Centre is sincerely appreciated. We would also like to express our sincere appreciation to the anonymous referee for valuable suggestions and corrections.

Conflicts of Interest: The authors declare no conflict of interest.

Appendix A

To facilitate the acquirement of data, the entire database has been uploaded to GitHub: <https://github.com/shenyx0126/Database-used-for-reliability-analysis.git> (accessed on 3 October 2022).

References

1. Kotsovos, M.D. Design for Punching of Flat Slabs. In *Compressive Force-Path Method*, 1st ed.; Springer: Berlin, Germany, 2014; Volume 5, pp. 83–107.
2. Yang, Y.Z.; Diao, M.Z.; Li, Y.; Guan, H.; Lu, X.Z. Post-punching failure mechanism and resistance of flat plate-column joints with in-plane constraints. *Eng. Fail. Anal.* **2022**, *138*, 106360. [CrossRef]
3. King, S.; Delatte, N.J. Collapse of 2000 Commonwealth Avenue: Punching Shear Case Study. *J. Perform. Constr. Facil.* **2004**, *18*, 54–61. [CrossRef]
4. Schellhammer, J.; Delatte, N.J.; Bosela, P.A. Another Look at the Collapse of Skyline Plaza at Bailey’s Crossroads, Virginia. *J. Perform. Constr. Facil.* **2013**, *27*, 354–361. [CrossRef]
5. Kinnunen, S.; Nylander, H. *Punching of Concrete Slabs without Shear Reinforcement*; KTH Royal Institute of Technology: Stockholm, Sweden, 1960.
6. Broms, C.E. Elimination of flat plate punching failure mode. *ACI Struct. J.* **2000**, *97*, 94–101.
7. Broms, C.E. Concrete Flat Slabs and Footings-Design Method for Punching and Detailing for Ductility. Ph.D. Thesis, KTH Royal Institute of Technology, Stockholm, Sweden, 2005.

8. Tian, Y.; Jirsa, J.O.; Bayrak, O. Strength Evaluation of Interior Slab-Column Connections. *ACI Struct. J.* **2008**, *105*, 692–700.
9. Stasio, D.; Buren, M.R.V. Transfer of Bending Moment between Flat Plate Floor and Column. *ACI J. Proc.* **1960**, *57*, 299–314.
10. Moe, J. *Shearing Strength of Reinforced Concrete Slabs and Footings under Concentrated Loads*; Portland Cement Association: Portland, Oregon, 1961.
11. MOHURD (Ministry of Housing and Urban-Rural Development of the People’s Republic of China). *GB 50010—2010 Code for Design of Concrete Structures*; China Architecture & Building Press: Beijing, China, 2015; pp. 232–236.
12. ACI (American Concrete Institute). *Building Code Requirements for Structure Concrete (ACI 318-19) and Commentary*; American Concrete Institute: Farmington Hills, MI, USA, 2019.
13. Muttoni, A. Punching shear strength of reinforced concrete slabs without transverse reinforcement. *ACI Struct. J.* **2008**, *105*, 440–450.
14. Wu, L.F.; Huang, T.C.; Tong, Y.L.; Liang, S.X. A Modified Compression Field Theory Based Analytical Model of RC Slab-Column Joint without Punching Shear Reinforcement. *Buildings* **2022**, *12*, 226. [[CrossRef](#)]
15. Chetchotiasak, P.; Ruengpim, P.; Chetchotsak, D.; Yindeesuk, S. Punching Shear Strengths of RC Slab-Column Connections: Prediction and Reliability. *KSCE J. Civ. Eng.* **2018**, *22*, 3066–3076. [[CrossRef](#)]
16. Nguyen, H.D.; Truong, G.T.; Shin, M. Development of extreme gradient boosting model for prediction of punching shear resistance of r/c interior slabs. *Eng. Struct.* **2021**, *235*, 112067. [[CrossRef](#)]
17. Mangalathu, S.; Shin, H.; Choi, E.; Jeon, J.S. Explainable machine learning models for punching shear strength estimation of flat slabs without transverse reinforcement. *J. Build. Eng.* **2021**, *39*, 102300. [[CrossRef](#)]
18. Chen, H.G.; Li, X.; Wu, Y.Q.; Zuo, L.; Lu, M.J.; Zhou, Y.S. Compressive Strength Prediction of High-Strength Concrete Using Long Short-Term Memory and Machine Learning Algorithms. *Buildings* **2022**, *12*, 302. [[CrossRef](#)]
19. Barkhordari, M.S.; Armaghani, D.J.; Mohammed, A.S.; Ulrikh, D.V. Data-Driven Compressive Strength Prediction of Fly Ash Concrete Using Ensemble Learner Algorithms. *Buildings* **2022**, *12*, 132. [[CrossRef](#)]
20. Shatnawi, A.; Alkassar, H.M.; Al-Abdaly, N.M.; Al-Hamdany, E.A.; Bernardo, L.F.A.; Imran, H. Shear Strength Prediction of Slender Steel Fiber Reinforced Concrete Beams Using a Gradient Boosting Regression Tree Method. *Buildings* **2022**, *12*, 550. [[CrossRef](#)]
21. Jiang, Y.M.; Li, H.Y.; Zhou, Y.S. Compressive Strength Prediction of Fly Ash Concrete Using Machine Learning Techniques. *Buildings* **2022**, *12*, 690.
22. Shen, Y.X.; Wu, L.F.; Liang, S.X. Explainable machine learning-based model for failure mode identification of RC flat slabs without transverse reinforcement. *Eng. Fail. Anal.* **2022**, *141*, 106647. [[CrossRef](#)]
23. Shen, Y.X.; Sun, J.H.; Liang, S.X. Interpretable Machine Learning Models for Punching Shear Strength Estimation of FRP Reinforced Concrete Slabs. *Crystals* **2022**, *12*, 259. [[CrossRef](#)]
24. Truong, G.T.; Hwang, H.J.; Kim, C.S. Assessment of punching shear strength of FRP-RC slab-column connections using machine learning algorithms. *Eng. Struct.* **2022**, *255*, 113898. [[CrossRef](#)]
25. Fu, B.; Feng, D.C. A machine learning-based time-dependent shear strength model for corroded reinforced concrete beams. *J. Build. Eng.* **2021**, *36*, 102118. [[CrossRef](#)]
26. Feng, D.C.; Ren, X.D.; Li, J. Stochastic damage hysteretic model for concrete based on micromechanical approach. *Int. J. Non-Linear Mech.* **2016**, *83*, 15–25. [[CrossRef](#)]
27. Chojaczyk, A.A.; Teixeira, A.P.; Neves, L.C.; Cardoso, J.B.; Soares, C.G. Review and application of Artificial Neural Networks models in reliability analysis of steel structures. *Struct. Saf.* **2015**, *52*, 78–89. [[CrossRef](#)]
28. Huang, B.Q.; Du, X.P. Probabilistic uncertainty analysis by mean-value first order Saddlepoint Approximation. *Reliab. Eng. Syst. Saf.* **2008**, *93*, 325–336. [[CrossRef](#)]
29. Feng, D.C.; Xie, S.C.; Li, Y.; Jin, L. Time-dependent reliability-based redundancy assessment of deteriorated RC structures against progressive collapse considering corrosion effect. *Struct. Saf.* **2021**, *89*, 102061. [[CrossRef](#)]
30. Xu, J.; Feng, D.C. Stochastic dynamic response analysis and reliability assessment of non-linear structures under fully non-stationary ground motions. *Struct. Saf.* **2019**, *79*, 94–106. [[CrossRef](#)]
31. Nassim, K.; Bouafia, Y.; Khalil, B. Reliability and punching shear resistance of slabs in non linear domain. *Gradevinar* **2016**, *67*, 1051–1062.
32. Olmati, P.; Sagaseta, J.; Cormie, D.; Jones, A.E.K. Simplified reliability analysis of punching in reinforced concrete flat slab buildings under accidental actions. *Eng. Struct.* **2017**, *130*, 83–98. [[CrossRef](#)]
33. Ricker, M.; Feiri, T.; Nille-Hauf, K.; Adam, V.; Hegger, J. Enhanced reliability assessment of punching shear resistance models for flat slabs without shear reinforcement. *Eng. Struct.* **2021**, *226*, 111319. [[CrossRef](#)]
34. Qiu, Z.P.; Huang, R.; Wang, X.J.; Qi, W.C. Structural reliability analysis and reliability-based design optimization: Recent advances. *Sci. China-Phys. Mech. Astron.* **2013**, *56*, 1611–1618. [[CrossRef](#)]
35. Rashki, M.; Ghavidel, A.; Arab, H.G.; Mousavi, S.R. Low-cost finite element method-based reliability analysis using adjusted control variate technique. *Struct. Saf.* **2018**, *75*, 133–142. [[CrossRef](#)]
36. Afshari, S.S.; Enayatollahi, F.; Xu, X.Y.; Liang, X.H. Machine learning-based methods in structural reliability analysis: A review. *Reliab. Eng. Syst. Saf.* **2022**, *219*, 108223. [[CrossRef](#)]
37. Wakjira, T.G.; Ebead, U.; Alam, M.S. Machine learning-based shear capacity prediction and reliability analysis of shear-critical RC beams strengthened with inorganic composites. *Case Stud. Constr. Mater.* **2022**, *16*, e01008. [[CrossRef](#)]

38. Deifalla, A. A comparative study and a simplified formula for punching shear design of concrete slabs with or without membrane tensile forces. *Structures* **2021**, *33*, 1936–1953. [[CrossRef](#)]
39. Xu, H.H.; Deng, Y. Dependent Evidence Combination Based on Shearman Coefficient and Pearson Coefficient. *IEEE Access* **2018**, *6*, 11634–11640. [[CrossRef](#)]
40. Feng, D.C.; Wang, W.J.; Mangalathu, S.; Taciroglu, E. Interpretable XGBoost-SHAP Machine-Learning Model for Shear Strength Prediction of Squat RC Walls. *J. Struct. Eng.* **2021**, *147*, 04021173. [[CrossRef](#)]
41. Salehi, H.; Burgueno, R. Emerging artificial intelligence methods in structural engineering. *Eng. Struct.* **2018**, *171*, 170–189. [[CrossRef](#)]
42. Chen, T.Q.; Guestrin, C. XGBoost: A Scalable Tree Boosting System. In Proceedings of the 22nd ACM SIGKDD International Conference on Knowledge Discovery and Data Mining (KDD), San Francisco, CA, USA, 13–17 August 2016.
43. Feng, D.C.; Wang, W.J.; Mangalathu, S.; Hu, G.; Wu, T. Implementing ensemble learning methods to predict the shear strength of RC deep beams with/without web reinforcements. *Eng. Struct.* **2021**, *235*, 111979. [[CrossRef](#)]
44. Liang, S.X.; Shen, Y.X.; Ren, X.D. Comparative study of influential factors for punching shear resistance/failure of RC slab-column joints using machine-learning models. *Structures* **2022**, *45*, 1333–1349. [[CrossRef](#)]
45. Rahman, J.; Ahmed, K.S.; Khan, N.I.; Islam, K.; Mangalathu, S. Data-driven shear strength prediction of steel fiber reinforced concrete beams using machine learning approach. *Eng. Struct.* **2021**, *233*, 111743. [[CrossRef](#)]
46. Mangalathu, S.; Karthikeyan, K.; Feng, D.C.; Jeon, J.S. Machine-learning interpretability techniques for seismic performance assessment of infrastructure systems. *Eng. Struct.* **2022**, *250*, 112883. [[CrossRef](#)]
47. Lundberg, S.M.; Lee, S.I. A Unified Approach to Interpreting Model Predictions. In Proceedings of the 31st Annual Conference on Neural Information Processing Systems (NIPS), Long Beach, CA, USA, 4–9 December 2017.
48. Lundberg, S.M.; Erion, G.; Chen, H.; DeGrave, A.; Prutkin, J.M.; Nair, B.; Katz, R.; Himmelfarb, J.; Bansal, N.; Lee, S.I. From local explanations to global understanding with explainable AI for trees. *Nat. Mach. Intell.* **2020**, *2*, 56–67. [[CrossRef](#)]
49. Yitzhaki, D. Punching strength of reinforced concrete slabs. *ACI J. Proc.* **1966**, *63*, 527–542.
50. Hawkins, N.M.; Fallsen, H.B.; Hinojosa, R.C. Influence of Column Rectangularity on the Behavior of Flat Plate Structures. *ACI Spec. Publ.* **1971**, *30*, 127–146.
51. Long, A.E. A Two-Phase Approach to the Prediction of the Punching Strength of Slabs. *ACI J. Proc.* **1975**, *72*, 37–45.
52. Regan, P.E. Symmetric punching of reinforced concrete slabs. *Mag. Concr. Res.* **1986**, *38*, 115–128. [[CrossRef](#)]
53. Tang, M.; Yi, W.J.; Liu, L.W. Investigation on seismic performance of interior slab-column connections subjected to reversed cyclic loading. *Earthq. Eng. Eng. Dynam.* **2019**, *39*, 109–121.
54. MOHURD (Ministry of Housing and Urban-Rural Development of the People’s Republic of China). *GB 50011—2010 Code for Seismic Design of Buildings*; China Architecture & Building Press: Beijing, China, 2016.
55. MOHURD (Ministry of Housing and Urban-Rural Development of the People’s Republic of China). *GB 50068—2018 Unified Standard for Reliability Design of Building Structures*; China Architecture & Building Press: Beijing, China, 2018.
56. Wakjira, T.G.; Ibrahim, M.; Ebead, U.; Alam, M.S. Explainable machine learning model and reliability analysis for flexural capacity prediction of RC beams strengthened in flexure with FRCM. *Eng. Struct.* **2022**, *255*, 113903. [[CrossRef](#)]
57. Shooman, M.L. *Probabilistic Reliability: An Engineering Approach*; McGraw-Hill: New York, NY, USA, 1986.
58. Hadianfard, M.A.; Malekpour, S.; Momeni, M. Reliability analysis of H-section steel columns under blast loading. *Struct. Saf.* **2018**, *75*, 45–56. [[CrossRef](#)]
59. Xia, Z.Y.; Quek, S.T.; Li, A.Q.; Li, J.H.; Duan, M.J. Hybrid approach to seismic reliability assessment of engineering structures. *Eng. Struct.* **2017**, *153*, 665–673. [[CrossRef](#)]
60. Strauss, A.; Hoffmann, S.; Wendner, R.; Bergmeister, K. Structural assessment and reliability analysis for existing engineering structures, applications for real structures. *Struct. Infrastruct. Eng.* **2009**, *5*, 277–286. [[CrossRef](#)]
61. Gesund, H.; Kaushik, Y.P. *Analysis of Punching Shear Failures in Slabs*; International Association for Bridge and Structural Engineering: Zurich, Switzerland, 1970; pp. 41–60.
62. Ramdane, K.E. Punching shear of high performance concrete slabs. In Proceedings of the 4th International Symposium on Utilization of High Strength/High Performance Concrete, Paris, France, 29 May 1996.
63. Xiao, R.Y.; Chin, C.S. Flat Slabs at Slab-Column Connection: Nonlinear Finite Element Modelling and Punching Shear Capacity Design Criterion. *Adv. Struct. Eng.* **2007**, *10*, 567–579. [[CrossRef](#)]